Journal of Materials Chemistry A

Accepted Manuscript

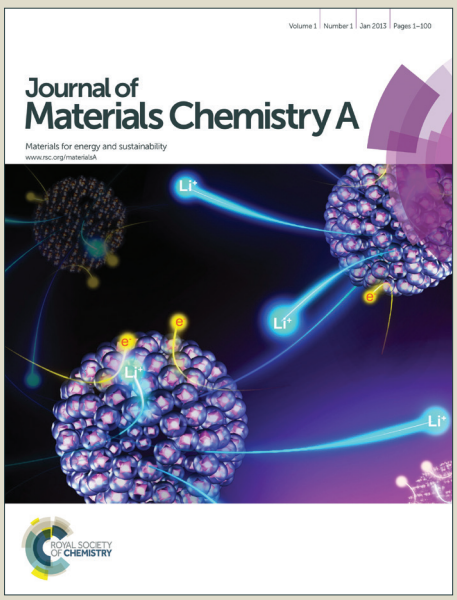

ROYAL SOCIETY OF CHEMISTRY

www.rsc.org/materialsA

Journal Name

COMMUNICATION

Synchronous synthesis of Si/Cu/C ternary nano-composite as Anode for Li Ion Batteries

Received 00th January 20xx,
Accepted 00th January 20xx

DOI: 10.1039/x0xx00000x

www.rsc.org/

Ning Lin[a], Jie Zhou[a], Jianbin Zhou[a], Ying Han[a], Yongchun Zhu[a*], and Yitai Qian[a*]

Commercial micron-sized bulk Si is chemically converted into nano-sized Si/Cu/C ternary composite. The Si particles, Cu crystals, and amorphous carbon are generated synchronously and mixed uniformly. As an anode, the Si/Cu/C exhibits a capacity of 1560 mAh g^{-1} after 80 cycles at 0.5 mA g^{-1}, long-term cycling stability with a capacity of 757 mAh g^{-1} at 2 A g^{-1} after 600 cycles, and fine rate capability.

Recently, silicon (Si) is considered as one promising anode material for the next generation of rechargeable lithium ion batteries (LIBs).[1] The high theoretical gravimetric capacity (3579 mAh g^{-1} for $Li_{15}Si_4$ alloy) and low working potential (<0.5 V vs Li/Li^+), associated with the abundant availability, are the significant advantages over other anode materials.[2] However, the large amount of Li ion alloying/de-alloying would cause huge volume contraction/expansion(~300%), leading to drastic cracking and the pulverization of the electrode during repetitive lithiation/delithiation process.[3] Once the interface between Si and current collector is disconnected, the specific capacity would fade rapidly.[4, 5]

To circumvent these issues, one feasible method is decreasing the size of the active materials. Various methods have been developed such as thermal decomposition of silane,[6] magnesiothermic reduction of silicon oxides,[7-8] reduction of $SiCl_4$ in inorganic solvent,[9] or via recently developed molten salts assisted reaction at 200 °C.[10] Other widely used approaches are generally realized by converting bulk Si or Si wafer into nanostructured Si materials through mechanical ball-milling or metal-assisted etching.[11-15] For example, J. Cho et al. produced Si nanowires by silver catalytic chemical etching of Si wafer in an hazardous etchant solution (10% HF and 1.2% H_2O_2), exhibiting a capacity of 1500 mA h g^{-1} at 300 mA g^{-1} after 50 cycles.[12] Nanostructure Si agglomerates, prepared by high-energy ball-milling micron-sized Si, delivered a capacity of 1170 mAh g^{-1} at 0.48 A g^{-1} over 600 cycles.[14] T. Wada et al. prepared three-dimensional nanoporous Si via dealloying Mg_2Si in a metallic Bi melt.[15]

The other well-accepted strategy is introducing an additive material to modify the Si.[16-24] Generally, carbonaceous materials and metals are considered as favorable additives due to their fine conductivity and the strong mechanical properties. For example, Y. Cui et al prepared carbon-silicon core-shell nanowires by deposition Si on carbon nanowires, which delivered a reversible capacity of ~2000 mAh g^{-1} at 0.5 A g^{-1} for 30 cycles.[17] Cu/Si films, fabricated via magnetron sputtering, delivered a capacity of 1100 mAh g^{-1} after the 100 cycles at 0.3 A g^{-1}.[23] Si-Mn/reduced graphene oxide composite synthesized by mechanical complexation and subsequent thermal reduction displayed a specific capacity of 600 mAh g^{-1} after 50 cycles at a current density of 100 mA g^{-1}.[24] Very recently, Our group reported a one-step metathesis reaction between Mg_2Si and GeO_2 which produced Si and Ge nano-composites.[25]

Inspired by the active Mg_2Si, in this study, a two-step method to chemically convert commercial micro-sized Si into a nano-sized silicon/copper/amorphous carbon ternary composite (Si/Cu/C) is developed, as exhibited in Scheme S1. First, Mg_2Si is pre-synthesized by alloying reaction between commercial Si and metallic Mg at 700 °C. Subsequently, a metathesis reaction between Mg_2Si and $Cu(CH3COO)_2{\cdot}H_2O$ is carried out at 450 °C. Note that Si, Cu and C contents are generated synchronously. The reaction can be described as: $4Mg_2Si + Cu(CH3COO)_2{\cdot}H_2O = 8\,MgO + 4Si + Cu + 2C + 4H_2$ (1). The by-products MgO is removed by diluted HCl solution without hazardous HF reagent. As anode for LIBs, the as-prepared Si/Cu/C composite shows a reversible capacity of 1560 mAh g^{-1} after 80 cycles at 0.5 A g^{-1}, long-term cycling stability with 757 mAh g^{-1} at 2 A g^{-1} after 600 cycles, and fine rate capability. However, the micro-sized bulk Si anode only retains a specific capacity of 233 mAh g^{-1} at 0.5 A g^{-1} after 80 cycles. The enhanced electrochemical performance could be attributed to following aspects. First, the generated Si with decreased particles size, which could effectively relax the strain stress, guarantees the high reversible capacity. Furthermore, the generated Cu and carbon, with good mechanical

[a] *Hefei National Laboratory for Physical Science at Micro-scale, Department of Chemistry, University of Science and Technology of China, Hefei, Anhui 230026, P. R. China. E-mail: ychzhu@ustc .edu.cn; ytqian@ust c.edu.cn*

† Electronic Supplementary Information (ESI) available: Experimental section; auxiliary analysis such as XRD, XPS images of the as-prepared samples. See DOI: 10.1039/x0xx00000x

and electrical properties, are beneficial for further accommodating of the volume change, and enhancing the electron/ion transfer.

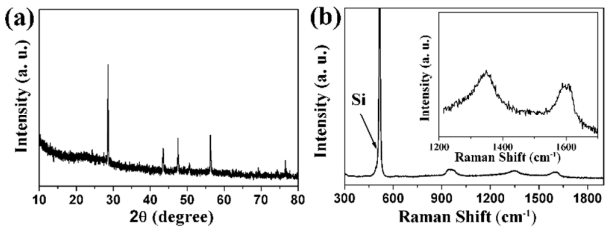

Figure 1. (a)The XRD patterns, and (b) The Raman spectrum of the Si/Cu/C composite.

X-ray powder diffractions (XRD) analysis is used to determine the phase of the final products, as shown in Figure 1a. The contents of final product obtained from the Reaction 1 is determined by XRD. The peaks at around 28.5, 47.5 and 56.3° are assigned to cubic phase Si (JCPDS No. 77-2111). The peaks located at 43 and 50.4 are the characterization peak of cubic phase copper (JCPDS No. 01-1242). The product is further analyzed by Raman spectrum, as shown in Figure 1b. The clear peak at 515 cm^{-1} corresponds to first-order Raman scattering from optic phonons of Si-Si stretching motions, suggesting the existence of Si component. Two broad peaks at 1340 and 1584 cm^{-1}, named as D band and G band of graphite, confirm the formation of carbon in the obtained composite. It should be mentioned that no obvious XRD diffraction patterns of carbon is observed. It is therefore presumed that the carbon generated in this reaction system is amorphous phase. The surface contents of the as-prepared nano-sized Si/Cu/C ternary composite is determined by X-ray photoelectron emission microscopy. The molar ratio of C, O, Cu and Si elements are estimated to be about 24: 48: 2: 26. (Figure S1)

The morphology and shape of the samples investigated by electron microscopy images. The commercial Si is composed of disordered bulk particles with the size up to few micro-meters (Figure 2a). The corresponding XRD patterns in Figure S2 shows that these particles are well-crystallized. Figure 2b exhibits the SEM picture of intermediate Mg_2Si. Clearly, the particles size of Mg_2Si becomes smaller than the raw bulk Si, displaying fused surface. Figure S2 presents the XRD patterns of the pre-synthesized Mg_2Si intermediate, all the peaks could be indexed to cubic phase Mg_2Si (JCPDS NO. 34-0458), implying the complete reaction between Si and metallic Mg at 700 °C.

After reacted with $Cu(CH_3COO)_2 \cdot H_2O$, the products possess aggregated particles with irregular morphology (Figure 2c). The corresponding TEM image (Figure 2d) shows that these particles are constructed by smaller basic particles that are interconnected with each other together. The high-resolution transmission electron microscopy (HR-TEM) image is also taken (Figure 3a). As we can see, the interplanar spacing of about 3.1 and 2.1 Å are attributed to the (111) planes of the crystalline Si and Cu, respectively.

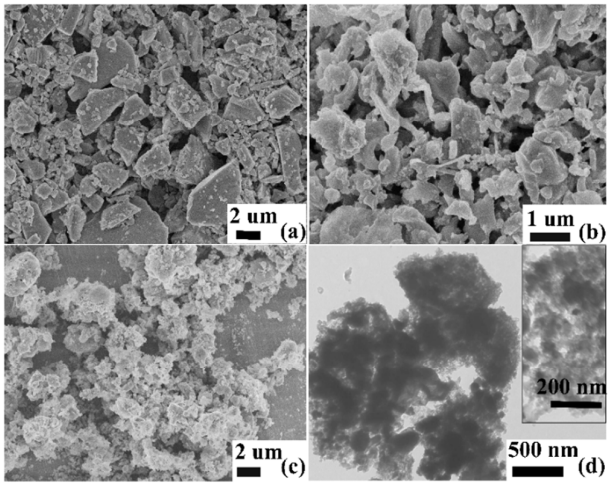

Figure 2. The SEM images of the (a) commercial bulk Si, (b) the as-prepared Mg_2Si, and (c) the Si/Cu/C composite. (d) The TEM picture of the Si/Cu/C composite.

These particles are contacted tightly. It could be detected that the amorphous phase may be assigned to the amorphous carbon. To further identify the elemental distribution of the prepared composite, energy dispersive X-ray (EDX) mapping images were taken. Figure 3c-d show the EDX mapping images for the Si, Cu, and C elements in the rectangular box of Figure 3b. It is clear that the three elements are uniformly distributed in the as-prepared composite. Above all, the commercial micro-sized bulk Si is converted into nano-sized Si/Cu/C ternary composite after the proposed two-step treatment. During the procedure, Si, Cu and C are generated synchronously, making sure of the uniform distribution of these components.

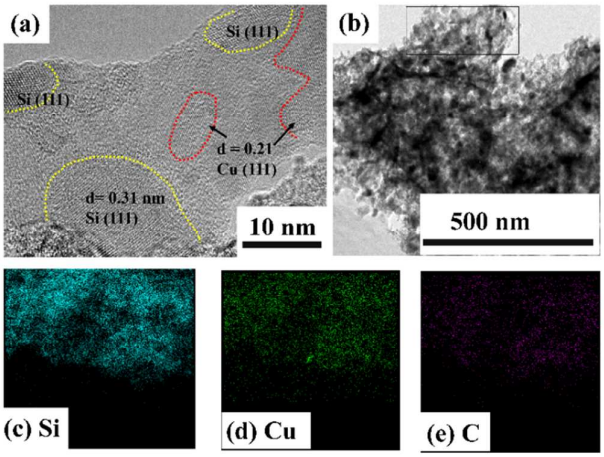

Figure 3. (a) The HRTEM image of the Si/Cu/C composite. The EDX mapping picture of (c) Si, (d) Cu, and (e) C elements.

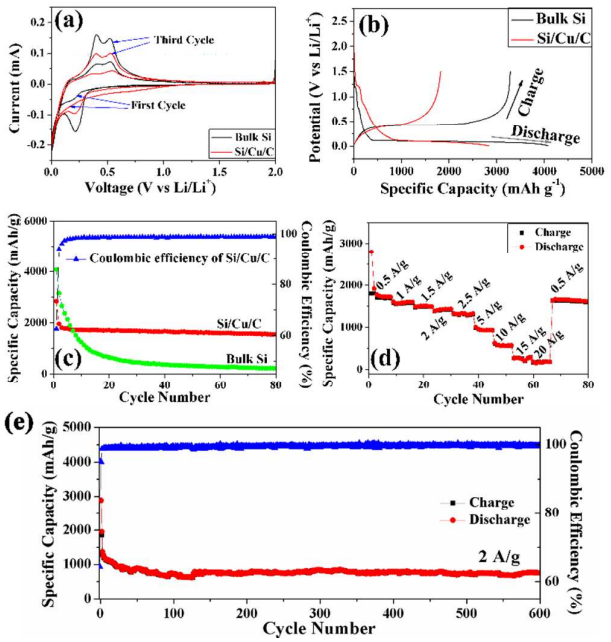

Figure 4. (a) The Cyclic voltammogram and (b) the initial voltage-capacity plots of bulk Si and the Si/Cu/C composite. (c) The discharge/charge cycling performance of the bulk Si and the Si/Cu/C composite at a current density of 0.5 A g^{-1}. (d) The rate capability of the Si/Cu/C composite with a current density ranging from 0.5 to 20 A g^{-1}. (e) Galvanostatic discharge/charge cycling at 2 A g^{-1} of the Si/Cu/C composite.

As anodes for LIBs, the electrodes fabricated by bulk Si raw materials and the as-prepared nano-sized Si/Cu/C ternary composite were tested in half cells with lithium foil as counter electrodes. The cyclic voltammetry (CV) measurement of bulk Si and as-prepared Si/Cu/C was carried out to determine the electrochemical reaction between the electrode and Li^+, as shown in Figure 4a. In the first cathode part, both bulk Si and Si/Cu/C exhibit the strong peak below 0.1 V, suggesting the alloying reaction between Si and Li^+.[26] In the first anode part, two peaks at 0.35 and 0.55 V (vs Li/Li^+) are corresponding to extraction of Li^+ from Li-Si alloy.[16] In the subsequent cycle, it should be noted that the cathode peaks change from 0.1 V (vs Li/Li^+) for the first cycle to higher potential at around 0.2 V (vs. Li/Li^+). Previous studies demonstrated that this variation is due to the amorphization process of crystalized Si during Li-alloying/de-alloying process.[14-15] Noteworthy, the characterization peaks corresponding Li-alloying and dealloying of bulk Si and Si/Cu/C are located at the same position. It is reasonable to speculate that the electrochemically active content in the Si/Cu/C composite is mainly attributed by Si.

The first charge-discharge curves of the electrodes are showed in Figure 4b. The initial discharge/charge capacity for bulk Si and Si/Cu/C electrodes are 4083/3293 and 2886/1857 mAh g^{-1}, respectively. The decrease of the first discharge capacity of Si/Cu/C may be caused by the electrochemically inactive component of Cu and the generated carbon with lower specific capacity. The initial coulombic efficiency (CE) of Si/Cu/C and bulk Si are 65% and 81%, respectively. The decrease of CE is mainly attributed to the improved specific surface of the nano-composite than that of bulk material and the silicon oxides formed during the treatment, which is more prone to result in the side reaction between the active material and electrolyte.

The cycling performance is evaluated by galvanostatic discharge/charge measurement, as shown in figure 4c. At a current density of 0.5 A g^{-1}, the Si/Cu/C exhibits a stable capacity retention behavior with a specific capacity of 1560 mAh g^{-1} after 80 cycles. However, despite the high initial discharge capacity of 4100 mAh g^{-1}, the bulk Si only retains a capacity of 233 mAh g^{-1} after 80 cycles. The drastic capacity decaying is mostly attributed to the cracking and pulverization of the bulk Si. Note that the CE of the Si/Cu/C increases from 65% for the first cycle rapidly to 96% for the second cycle, and maintains stable at about 99% in the subsequent cycles.

Furthermore, to evaluate the rate capability, the Si/Cu/C are tested with increasing current density from 0.5 to 20 A g^{-1}. The Si/Cu/C electrode exhibits average capacity of 1743, 1573, 1506, 1430, 1337, 942, 577, 273, and 173 mAh g^{-1} at the current density of 0.5, 1, 1.5, 2, 2.5, 5, 10, 15, and 20 A g^{-1}, respectively. As the current density returned back to 0.5 A g^{-1}, a reversible capacity as high as 1638 mAh g^{-1} is restored even after cycling at high current density, indicating fine rate capability.

In addition, long cycling stability is tested at 2 A g^{-1}, as shown in Figure 4e. After 60 cycles, the specific capacity of Si/Cu/C decreases to 760 mAh g^{-1}. But, from 60th cycle forward, no remarkable capacity fading is detected. The reversible capacity still retains 754 mAh g^{-1} even over 600 cycles. Note that the first two charge/discharge cycles are tested at relatively low current density of 0.2 A g^{-1} in order to active the electrode sufficiently.

The electrochemical impedance spectrum (EIS) is measured to investigate the charge transport kinetics for the electrochemical properties of these electrodes. Figure 5 shows the experimental and the fitted Nyquist plots of Si/Cu/C nano-composite and commercial bulk Si electrodes, associated with the equivalent Randles circuit. These curves are composed of depressed semicircles in the high frequency range and low frequency sloping lines. The analysis and the fitted data for all circuit elements is exhibited in Supporting Information. The R_{CT}, which is known as charge transfer resistance in the electrode/electrolyte interface, [27, 28] of bulk Si and Si/Cu/C electrode is 282 and 120 Ω, respectively. Obviously, the bulk Si electrode shows considerably higher layer resistance than that of the Si/Cu/C electrode. The W (Warburg element) indicates that the Si/Cu/C electrode exhibits higher ion diffusion coefficient compared with bulk Si electrode. It is reasonable to conclude that the conductive Cu and C components is able to improve the electron transfer from embedded Si nanoparticles within the whole electrode, and thus decreases the resistance. The electrode morphology (Figure S3) shows that the electrode surface becomes smoother after cycling, which may be resulted from the formation of SEI membrane. Note that the Si/Cu/C based electrode still presents flat surface. But, the bulk Si electrode exhibits obvious protuberance on the surface, which may be caused by the huge volume change of the micro-sized bulk Si.

Compared with commercial bulk Si electrode, the nano-sized Si/Cu/C ternary composite exhibits the high reversible capacity, long-term cycling stability, and fine rate capability. The enhanced performance of Si/Cu/C ternary composite may be attributed to the

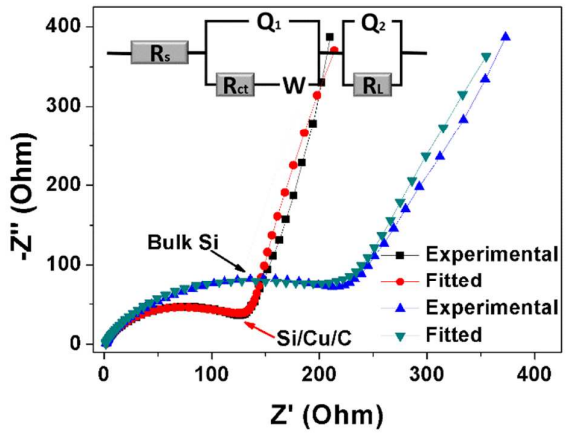

Figure 5. The experimental and fitted Nyquist plots of the bulk Si and the Si/Cu/C composite. The equivalent Randles circuit is shown in the inset.

following aspects. On the one hand, the nano-sized Si particles, evolved from commercial micro-Si, acted as main active material to react with Li^+ reversibly, guaranteeing the high reversible capacity. The decreased particle size could effectively relax the strain stress, keeping the electrode integrity. On the other hand, the Cu and amorphous carbon components could serve as protective matrix for further buffering the volume change. And that are the key features for improving the cycling stability with high specific capacity of Si-based anode. Furthermore, the generated Cu and carbon, with fine conductivity, is beneficial for enhancing the fast charge/discharge test, leading to fine rate capability.

Conclusions

In summary, a safe two-step strategy converting commercial micro-sized bulk Si into nano-sized Si/Cu/C ternary composite is proposed. During the procedure, the Si particles, Cu crystals, and amorphous carbon contents in the composite are generated synchronously and mixed uniformly. As anode for LIBs, the as-prepared Si/Cu/C displays enhanced electrochemical performance than bulk Si. Fundamentally, the Si contribution is the main active material offering a high reversible capacity. In the composite, the Cu and C components could not only act as a protective matrix for accommodating the volume change of Si, but also facilitate the electronic/ionic conductivity. As a result, when used as anode for LIBs, the Si/Cu/C anode exhibits reversible capacity of 1560 mAh g^{-1} at 0.5 A g^{-1} after 80 cycles, long-term cycling stability, and fine rate capability. This chemical strategy without using any hazardous reagents such as HF opens up a new way for using low-cost bulk Si.

Acknowledgements

This work was financially supported by the 973 Project of China (No. 2011CB935901), the National Natural Science Fund of China (No. 21471142, 21201158).

Notes and references

1 S. Choi, J. C. Lee, O. Park, M-J. Chun, N-S. Choi and S. Park, *J. Mater. Chem. A*, 2013, **1**, 10617-10621.
2 Y. L. Wang, T. Y. Wang, P. M. Da, M. Xu, H. Wu and G. F. Zheng, *Adv. Mater.*, 2013, **25**, 5177-5195.
3 J. Y. Choi, D. J. Lee, Y. M. Lee, Y. G. Lee, K. M. Kim, J. K. Park, and K. Y. Cho, *Adv. Funct. Mater.*, 2013, **23**, 2108-2114.
4 W. F. Ren, Z. L. Zhang, Y. H. Wang, Q. Q. Tan, Z. Y. Zhong, and F. B. Su, *J. Mater. Chem. A,* 2015, **3**, 5859-5865.
5 B. Liang, Y. P. Liu, and Y. H. Xu, *J. Power Sources*, 2014, **267**, 469-490.
6 C. K. Chan, H. L. Peng, G. Liu, K. Mcilwrath, X. F. Zhang, R. A. Huggins, and Y. Cui, *Nat. Nanotechnol*., 2008, **3**, 31-35.
7 A. Xing, J. Zhang, Z. H. Bao, Y. F. Mei, A. S. Gordin and K. H. Sandhage, *Chem. Commun*., 2013, **49**, 6743-6745.
8 H. P. Jia, P. F. Gao, J. Yang, J. L. Wang, Y. Nuli, and Z. Yang, *Adv. Energy Mater*., 2011, **1**, 1036–1039.
9 H. Kim, M. Seo, M. H. Park, and J. Cho, *Angew. Chem. Int. Ed*., 2010, **49**, 2146–2149.
10 N. Lin, Y. Han, L. B. Wang, J. B. Zhou, J. Zhou, Y. C. Zhu, and Y. T. Qian, *Angew. Chem. Int. Ed.*, 2015, **54**, 3822-3825.
11 M. Y. Ge, J. P. Rong, X. Fangand C. W. Zhou, *Nano Lett.,* 2012, **12**, 2318–2323.
12 B. M. Bang, H. Kim, J-P. Lee, J. Cho, and S. Park, *Energy Environ. Sci.*, 2011, **4**, 3395–3399.
13 Z. Zhang, Y. Wang, W. Ren, Q. Tan, Y. Chen, H. Li, Z. Zhong and F. Su, *Angew. Chem. Int. Ed.*, 2014, **53**, 5165-5169.
14 M. Gauthier, D. Mazouzi, D. Reyter, B. Lestriez, P. Moreau, D. Guyomard, and L. Rou'e, *Energy Environ. Sci.*, 2013, **6**, 2145–2155.
15 Z. L. Zhang, Y. H. Wang, W. F. Ren, Q. Q. Tan, Y. F. Chen, H. Li, Z. Y. Zhong, and F. B. Su, *Angew. Chem.*, 2014, **126**, 5265-5269.
16 N. Lin, J. B. Zhou, L. B. Wang, Y. C. Zhu, and Y. T. Qian, *ACS Appl. Mater. Interfaces,* 2015, **7**, 409–414.
17 L. F. Cui, Y. Yang, C. M. Hsu and Y. Cui, *Nano Lett.*, 2009, **9**, 3370-3374.
18 S-O. Kim and A. Manthiram, *J. Mater. Chem. A*, 2015, **3**, 2399–2406.
19 B.D. Polat, O. Keles, *J. Alloy. Compd.*, 2015, **622**,418–425.
20 S. Murugesan, J. T. Harris, Brian A. Korgel, and K. J. Stevenson, *Chem. Mater.*, 2012, **24**, 1306-1315.
21 J. Xie, X. G. Yang, S. Zhou, and D. W. Wang, *ACS Nano*,2011, **5**,9225-9231.
22 S. Guo, H. X. Li, H. M. Bai, Z. L. Tao, and J. Chen, *J. Power Sources,* 2014, **248**,1141-1148.
23 Y. He, Y. H. Wang, X. Q. Yu, H. Li, and X. J. Huang, *J. Electrochem. Soc.*, 2012, **159**, A2076-A2081.
24 A. R. Park, J. S. Kim, K. S. Kim, K. Zhang, J. Park, J. H. Park, J. K. Lee, and P. J. Yoo, *ACS Appl. Mater. Interfaces*, 2014, **6**, 1702-1708.
25 N. Lin, L. Wang, J. Zhou, J. Zhou Y. Han, Y. Zhu, Y. Qian, and C. Cao, *J. Mater. Chem. A*, 2015, **3**, 11199-11202.
26 N. Lin, J. B. Zhou, Y. C. Zhu and Y. T. Qian, *J. Mater. Chem. A*, 2014, **2**, 19604–19608.
27 W. Wang, S. Guo, I. Lee, K. Ahmed, J. Zhong, Z. Favors , F. Zaera, M. Ozkan, C. S. Ozkan, *Sci. Rep.*, 2014, 4:4452.
28 Y. Zhu, Y. Xu, Y. Liu, C. Luo, C. Wang, *Nanoscale*, 2013, **5**,780–787.

Synchronous synthesis of Si/Cu/C ternary nano-composite as Anode for Li Ion Batteries

Ning Lin[a], Jie Zhou[a], Jianbin Zhou[a], Ying Han[a], Yongchun Zhu[a], Yitai Qian[a]

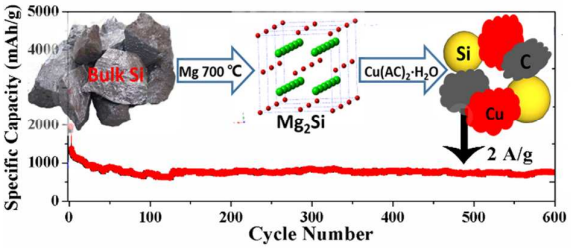

Commercial micron-sized bulk Si is chemically converted into nano-sized Si/Cu/C ternary composite as anode material. The Si particles, Cu crystals, and amorphous carbon are generated synchronously and mixed uniformly.